NASA Contractor Report 156844

# Detailed Gravity Anomalies from GEOS-3 Sateilite Altimetry Data



G.S. Gopalapillai and A.G. Mourad

October 1978



NASA
National Aeronautics and Space Administration

**Wallops Flight Center**
Wallops Island, Virginia 23337
AC 804 824-3411

## FORWARD

This investigation was performed by Battelle's Columbus Laboratories (BCL) for the National Aeronautics and Space Administration (NASA), Wallops Flight Center (WFC), Wallops Island, Virginia, under Contract No. NAS6-2801. Mr. H. Ray Stanley served as the NASA Technical Monitor.

The excellent cooperation of Professor Richard H. Rapp of the Ohio State University is gratefully acknowledged. As one of the GEOS-3 Principal Investigators, he provided all of the processed altimetry data in the calibration area, most of them even before publication. He also made available the terrestrial gravity data and a few computer subroutines. Mr. James Marsh of the NASA/Goddard Space Flight Center supplied the GEM-9 potential coefficients set.

## EXECUTIVE SUMMARY

The objective of this investigation was to develop methods and procedures that could be used in establishing practical applications for the high resolution altimeter capability of the GEOS-3 and future SEASAT satellite missions. The geopotential model that has direct applications in several areas of geophysics, marine geodesy, oceanography, Earth resources, etc., is the free air gravity anomaly. The requirements for gravity anomalies in potential application areas such as oil and gas exploration are highly demanding in terms of accuracy and resolution. Consequently, Battelle's effort was directed toward development and test of a suitable technique for deriving mean gravity anomalies from dense altimetry data to a resolution that has not been achieved before. Obviously, the achievement of such a resolution has to be approached on a non-global basis.

The procedure developed and applied in this study uses a combination of both deterministic and statistical techniques. The basic mathematical model was based on the Stokes' equation which describes the analytical relationship between mean gravity anomalies and geoid undulations at a point; this undulation is a linear function of the altimetry data at that point. The overdetermined problem resulting from the excessive altimetry data available was solved using Least-Squares principles. These principles enable the simultaneous estimation of the associated standard deviations reflecting the internal consistency based on the accuracy estimates provided for the altimetry data as well as for the terrestrial anomaly data.

Using GEOS-3 data in the calibration area, several test computations were made of the anomalies and their accuracy estimates for different combinations of:

(1) Four a priori weighting functions for anomaly parameters

(2) Two anomaly parameter configurations

(3) Three data densities and distributions.

For "profile" type or low density data, the computed anomalies were sensitive to the a priori weights. For such a distribution of data, numerical anomaly auto- and cross-covariance functions can be used as weighted constraints to obtain realistic estimates for anomalies and their accuracies.

Computed anomalies for 1° x 1° blocks were compared with terrestrial estimates and also with a set of anomalies computed by Rapp using Least-Squares Collocation procedures. The RMS differences were 8.7 mgal and 5.4 mgal, respectively, which were consistent with accuracy estimates associated with these sets (10 mgal for terrestrial data and 7.3 mgal for Rapp's data).

The accuracy estimates for 1° x 1° mean anomalies that can be obtained with the techniques used in this study are of the order of 2 mgal, which is at least about four times better than the estimates for the terrestrial data and Rapp's data. Estimation of 30' x 30' anomalies can be accomplished with accuracies of about 5 mgal using the techniques employed here. These accuracy figures are very encouraging, indicating the potential applications of the altimeter data in a variety of areas. As a result of the lack of accurate ground truth data, proper verification of the fine results obtained by the procedures developed and used here is not possible. This situation emphasizes the pressing need for a marine test range where detailed and accurate ground truth gravity data would be collected and made available to verify the results of GEOS-3 altimetry data and also of further improved data expected of the future SEASAT satellite missions.

TABLE OF CONTENTS



LIST OF TABLES

## LIST OF TABLES
(Continued)



## LIST OF FIGURES

# DETAILED GRAVITY ANOMALIES FROM GEOS-3 SATELLITE ALTIMETRY DATA

by

G. S. Gopalapillai and A. G. Mourad

## 1. INTRODUCTION

This report covers activities performed by Battelle's Columbus Laboratories (BCL) for the National Aeronautics and Space Administration, Wallops Flight Center, under Contract No. NAS6-2801. The primary objective of these activities is the development and testing of a suitable technique for estimating the fine structure of the Earth's gravity field from the high resolution altimeter capability of GEOS-3 and future SEASAT satellite missions.

With the successful launch and operation of the Skylab and GEOS-3 satellite altimeter systems, the acquisition of detailed gravity data over the vast oceans of the Earth experienced a quantum jump in speed and detail. Those data are directly derived from the altimetry measurements in the form of geoid undulations which describe the separation of the geopotential level surface corresponding to the Mean Sea Level (MSL) and the reference ellipsoid adopted as the closest analytical surface representing the Earth.[1]* However, the geopotential model that has direct applications in several areas of geophysics, marine geodesy, oceanography, Earth resources, etc., is the free air gravity anomaly. The advantage of the gravity anomaly model over the undulation model is its higher sensitivity to the various (anomalous) features on or near the Earth's surface. Further, the direct observations of the gravity on the Earth's surface lend themselves to the natural representation of the anomalous geopotential field by free air gravity anomalies.

The requirements for gravity anomalies in potential application areas such as oil and gas exploration are highly demanding in terms of accuracy and resolution. The unprecedented resolution and speed with which the altimeter data have become available have resulted in the possibility that the fine structure (short wavelength features) of the anomalous

---

* References, denoted by superscript numbers, are at end of report in Section 7.

geopotential could be determined. The determination of this fine structure has a practical disadvantage where the number of geopotential parameters to be determined is too large to handle, even with the largest computer available today. Obviously, the possibilities for solution to this problem can only be achieved through use of some form of non-global solution.

Several methods and procedures can be found in the literature for determining gravity anomalies from altimetry data on a non-global basis. Some of these are purely deterministic and some are statistical, while others use a combination of these techniques. Examples of the statistical techniques are Least-Squares Collocation[2] and Fourier transform solutions[3]. A direct determination of point anomalies from altimeter data using the inverse Stokes' equation[4] is an example of the deterministic approaches[1,5].

The technique preferred over the above and employed in the ensuing study is a combination type using the analytical relationship (Stokes' equation)[6] between mean gravity anomalies and geoid undulation which is linearly related to the altimetry observation. This technique has several favorable features. The overdetermined problem resulting from the excessive altimetry data available can be solved using Least-Squares principles. Any a priori information available on the gravity anomalies being computed can be incorporated simultaneously using weighted constraints. Further, any systematic errors inherent in the altimetry data can be modeled and filtered out.

This method was developed and some simulation studies made while the principal author was working on an Air Force contract. The details of that work can be found in Reference(1). In the current study, essentially the same procedure, with minor modifications, is implemented with real altimetry data from GEOS-3. For the sake of completeness, a brief summary of the procedure is presented in Section 2, followed by a short description of the various data sets (altimetry as well as terrestrial gravity and potential coefficients) used (Section 3). In Sections 4 and 5, results are given for the 1° x 1° and 30' x 30' gravity anomaly determinations. Conclusions from these results and recommendations toward any future work in this area are presented in Section 6.

## 2. MATHEMATICAL MODEL AND PROCEDURE

As indicated earlier, the details of the technique and procedure used in this study are fully documented[1]. However, for the sake of completeness, the portions relevant to the mathematical model and the procedures for implementing the same will be summarized here.

### 2.1 Mathematical Model

For practical implementation, the Stokes' formula, generalized to any geocentric reference ellipsoid, can be written in the form:[1]

$$N_p = N_o + \frac{R}{4\pi G} \sum_i \sum_j \Delta g_{ij} \, S(\psi_{ij}) \, \Delta\sigma_{ij} \, , \qquad (1)$$

where

$N_p$ - undulation at point p

$N_o$ - scale constant

R - average Earth radius

G - average gravity on Earth

$\Delta g$ - free-air gravity anomaly

$\Delta\sigma$ - area of the block over which $\Delta g$ is assumed constant

$\psi_{ij}$ - distance between P and $\Delta\sigma$

ij - subscript identifying the block on a gridded format,

and $S(\psi_{ij})$ is the Stokes' function given as[6]:

$$S(\psi_{ij}) = \frac{1}{x} - 6x + 1 - 5\cos\psi_{ij} - 3\cos\psi_{ij} \ln(x + x^2) \, , \qquad (2)$$

with

$$x = \sin\left(\frac{\psi_{ij}}{2}\right) \, .$$

Equation (1) implies that $\Delta g$ and $N_p$ are compatible with respect to the flattening of the reference ellipsoid. It also implies that $\Delta g$ be known in every block ij on the Earth. However, the behavior of the kernel $S(\psi)$ in Equation (1) is such that it suppresses the effect of the gravity anomalies in the zones remote from the computation point so that only the lower harmonics of the gravity field in these areas contribute significantly to $N_p$. The lower degree harmonics are reasonably well known and may be used to advantage to compute the contribution from the zones remote from $N_p$.

In view of the above, the undulation $N_p$ can be assumed to be composed of four components, $N_o$, $N_1$, $N_2$ and $N_3$ such that:

$$N_p = N_o + N_1 + N_2 + N_3 \ , \tag{3}$$

where $N_1$, the lower harmonic contribution over the whole surface of the Earth, is given by:

$$N_1 = R \sum_{n=2}^{N_{max}} \sum_{m=0}^{n} (\bar{C}_{nm} \cos m\lambda + \bar{S}_{nm} \sin m\lambda)\, \bar{P}_{nm}(\sin\phi) \ , \tag{4}$$

with $(\phi,\lambda)$ = geocentric coordinates of P

$\bar{C}_{nm}$, $\bar{S}_{nm}$ = fully normalized potential coefficients referred to the same reference field to which $N_p$ in Equation (1) refers

$N_{max}$ = maximum degree to which potential coefficients are used

$P_{nm}(\sin\phi)$ = fully normalized associated Legendre function.

Then, $N_2$, the higher harmonic contribution from a cap centered at the computation point is expressed as:

$$N_2 = \frac{R}{4\pi G} \iint_{\sigma_c} (\Delta g - \Delta g_s) S(\psi)\, d\sigma \ , \tag{5}$$

with[7]

$$\Delta g_s = G \sum_{n=2}^{N_{max}} (n-1)\, \beta \sum_{m=0}^{n} \left[ \bar{C}_{nm} \cdot \frac{1}{A} \iint_A P_{nm} \cos m\lambda \, d\sigma \right.$$

$$\left. + \bar{S}_{nm} \cdot \frac{1}{A} \iint_A \bar{P}_{nm} \sin m\lambda \, d\sigma \right] , \tag{6}$$

where the smoothing operator $\beta$ is set to one. The integrals in Equation (6) indicate that $\Delta g_s$ is the mean gravity anomaly over the block of area A. $\sigma_c$ in Equation (5) implies that the integration is carried out w[illegible] spherical

cap of radius $\psi_o$. Then, the higher harmonic contribution from the area outside the cap is:

$$N_3 = \frac{R}{4\pi G} \iint_{\sigma-\sigma_c} (\Delta g - \Delta g_s) S(\psi) d\sigma \quad , \tag{7}$$

with $\sigma-\sigma_c$ being the area of the remote zones.

$N_3$ would be the error in $N_p$ if the actual anomaly information in the remote zones is replaced by anomalies implied by a spherical harmonic potential coefficient set truncated at degree $N_{max}$. Neglecting $N_3$ Equation (3) with Equation (5) can be written in the form:

$$N_p = N_o + N_1 + \frac{R}{4\pi G} \iint_{\sigma_c} \delta g \; S(\psi) \; \Delta\sigma \quad , \tag{8}$$

where $$\delta g = \Delta g - \Delta g_s \quad , \tag{8A}$$

which can be interpreted as the mean anomalies referred to a reference spherop of degree and order $N_{max}$.

At this point we have the option of modeling any systematic errors that may be inherent in the altimetry observations. However, the data we used in this study have been preprocessed and corrected for any systematic errors due to tides, orbit uncertainties, etc.[8]. Consequently, it is assumed that the data are free of systematic errors, other than the global constant parameter $N_o$, which can absorb any bias, constant over the area under consideration.

## 2.2 Procedure For Anomaly Recovery

The mathematical model expressed by Equation (8) forms the basis for the computation of mean gravity anomalies from altimeter data which, at this point, are assumed to be in the form of geoid undulations averaged over the radar footprints. Every altimeter observation will result in an equation of the type (8). Conceptually, a set of such equations will give a meaningful solution when the number of observations equals or exceeds the number of unknowns (anomalies and $N_o$).

In order to incorporate the a priori information, if any, on some or all unknowns, let all the unknowns also be treated as observables with a priori weights. Zero weights can be assigned to those unknowns for which no information is available. In this case, Equation (8) can be interpreted as a condition among observables. For consideration of redundancy, the number of observations would be the sum of the altimetry observations and the unknowns with non-zero weights. The resulting redundancy in the system can be exploited in some type of adjustment technique.

The mathematical model as given by Equation (8) can be rewritten in a more general form as follows:

$$F(N, \delta g, N_o) = 0 \ , \tag{9}$$

where F is a function of the altimetry observations N, the residual anomalies referred to a spherop of degree $N_{max}$, and the constant bias as expressed by Equation (8). In matrix notation, let $X_o$ denote the vector of a priori estimates of the unknowns ($\delta g$, $N_o$) and $N_{OB}$ be the vector of observed values of observables (N). If the adjusted values of these quantities are, respectively, $X^a$ and $N^a$, then:

$$\begin{aligned} X^a &= X_o + V_x \\ N^a &= N_{OB} + V_N \end{aligned} \ , \tag{10}$$

where $V_x$ and $V_N$ are vectors of residuals of the unknowns and observations, respectively.

Linearizing Equation (9), the resulting condition equation, in matrix notation, is:

$$V_N + AV_x + W = 0 \ , \tag{11}$$

where A is the design matrix of partial derivatives of F with respect to the unknowns. W is the misclosure vector obtained by evaluating F with the values $X_o$ and $N_{OB}$. If the weight matrices for the observations and unknowns (also considered observables) are P and $P_x$, respectively, then the Least-Squares solution for the residual vectors is:

$$V_x = - (A^T P A + P_x)^{-1} A^T P W \tag{12}$$

$$V_N = - (A V_x + W) \quad , \tag{13}$$

and the covariance matrix can be estimated from:

$$\Sigma_x = \sigma_o^2 (A^T P A + P_x)^{-1} \quad , \tag{14}$$

where $\sigma_o^2$ is the variance of unit weight estimated from

$$\sigma_o^2 = (V_N^T P V_N + V_x^T P_x V_x)/DF \quad , \tag{15}$$

with DF being the number of degrees of freedom.

The adjusted values of the unknowns and the observations are obtained by substituting the vectors $V_x$ and $V_N$ in Equation (10). The adjusted values of the anomalies are referred to the spherop of degree $N_{max}$. If the anomalies need to be referred to an ellipsoidal reference field, they can be obtained by simply adding $\Delta g_s$ [Equation (6)] back [Equation (8A)].

## 2.3 Non-Global Solution

The discussion thus far has been on the general feasibility of recovering gravity anomalies from altimetry data. The application of the above method for small regions of the Earth will be discussed here. In fact, the insignificant contribution to the geoid undulation at any point from anomalies in the remote zones is the key to this non-global solution.

Suppose that the anomalies within a given area, for example a circle of radius $\psi(I)$ centered at a point, Q, are to be determined. Then, the altimetry data within an area of a concentric circle (II) of radius $(\psi+\psi_{OM})$ are necessary to determine these anomalies so that the contribution

from altimetry data outside this circle is less than a predetermined value $\sigma_{OM}$. Figure 1 illustrates this system. Further, the mathematical model [Equation (8)] requires that the area of anomalies be extended to a further distance of $\psi_{OS}$ from Circle II to Circle III. This means there is no observation equation for any observation within Circle II that will have a cap extending beyond Circle III. At this point, it should be emphasized that although all the anomalies within Circle III will be treated as unknowns in this procedure, only for those within Circle I have all contributing factors been taken into account. This means that the determination of only those anomalies in Circle I can be totally reliable. The rest of the anomalies will be poorly determined and their quality of determination will deteriorate as the distance of these anomalies from Circle I increases.

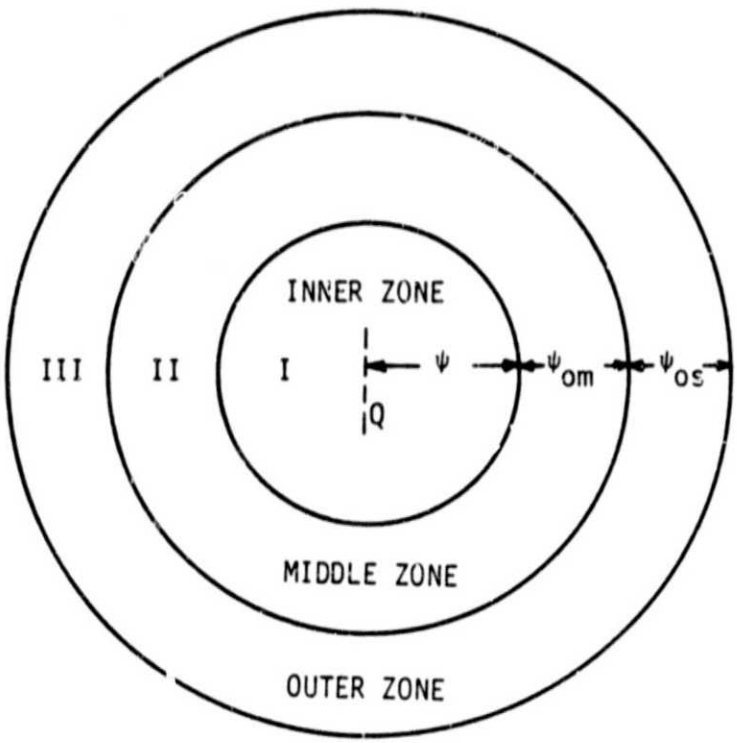


FIGURE 1. SYSTEM OF OBSERVATION AND UNKNOWNS FOR A NON-GLOBAL SOLUTION

Before proceeding further, we should define the angles $\psi_{OM}$ and $\psi_{OS}$ which determine the size of the circles. $\psi_{OM}$ is the size of the cap where the geoid undulations outside this cap have insignificant contribution to the anomaly at the center of the cap to a given accuracy level. This cap size can be determined by considering a graph of the remote-zones contributions to the anomaly through the Inverse-Stokes' formula for different cap sizes.[1] Then, for a given error of commission due to neglect of the remote-zone effects, the corresponding cap size can be interpolated from the graph. Incidentally, the subscript M indicates the cap size $\psi_0$ for Molodenskii's formula. Similarly, the subscript S in $\psi_{OS}$ denotes the cap size for Stokes' formula, and $\psi_{OS}$ can also be determined in the same fashion as $\psi_{OM}$.[1]

## 2.4 Evaluation of Stokes' Formula

In computing the elements of the design matrix A [Equation (11)], an average value of the Stokes' function as given by Equation (2) has to be evaluated for every anomaly block involved in the adjustment. Theoretically, the average value $\bar{S}(\psi)$ is expressed by:

$$\bar{S}(\psi) = \frac{1}{\Delta\sigma} \iint_{\Delta\sigma} S(\psi) d\sigma \quad . \tag{16}$$

However, in practice, Equation (16) is evaluated by computing one or several values of $S(\psi)$ for different points in the block in which the anomaly is given and averaging the results. The accuracy of this average will depend on the size of $\psi$ and the number of values computed. Since $S(\psi)$ is very sensitive for small values of $\psi$, more points are required for an accurate mean when $\psi$ is small than when $\psi$ is large. Rapp and Rummel have suggested the following guidelines for subdividing a $1^\circ \times 1^\circ$ block in evaluating Equation (16):[9]

$\psi \leq 2^\circ$: 64 sub-blocks
$2^\circ < \psi \leq 5^\circ$: 16 sub-blocks
$5^\circ < \psi \leq 10^\circ$: 4 sub-blocks
$10^\circ < \psi \leq 20^\circ$: 1 sub-block .

However, this system of subdivision has a weakness when used with altimetry data. That is, when the computation point coincides with the center of the sub-block (i.e., $\psi$=0), $S(\psi)$ will be singular. To overcome the singularity in the sensitive range of $\psi$, an alternative technique developed by Levallois[10] is used. Here, the geodetic coordinates are transformed into Cartesian coordinates using Mercator projection and the integration required for averaging $S(\psi)$ is carried out analytically. The details of this technique can be found in Reference (1).

The number of times the Stokes' function is evaluated may be as many as tens of thousands, considering the large number of altimeter observations, the anomaly blocks involved and the subdivision schemes used. It has been suggested[11] that it is economical, with respect to computer time, to do a linear interpolation in a table of about 150 values of $S(\psi)$ rather than to evaluate them from Equation (2). However, the Stokes' function is too sensitive for such interpolation in the range of $\psi$(0° to 20°) involved in the study. This sensitivity problem could be overcome by modifying the procedure as follows.

The function $F(\psi)$ defined as:

$$F(\psi) = \frac{\sin \psi}{2} S(\psi) \quad , \tag{17}$$

is known to be stable for values of $\psi$ within the range under consideration.[6] Therefore, the values of $F(\psi)$, instead of $S(\psi)$, are tabulated. Then the value of $F(\psi)$ for a given value of $\psi$ is obtained by linearly interpolating between the tabulated values, and the corresponding $S(\psi)$ is simply obtained using Equation (17).

The values of $F(\psi)$ are tabulated as follows, with the values of $\psi$ in degrees:

For $0.1 < \psi < 1$ at every hundreth of a degree

$1 < \psi < 5$ at every tenth of a degree

$\psi > 5$ at every degree

$\psi < 0.1$ a constant value of 1.0007 is used[11].

## 3. DATA DESCRIPTION

The various types of data used in this study are described here. These include:

(1) Altimetry data

(2) Terrestrial anomaly data

(3) Spherical harmonic potential coefficients set

(4) Numerical auto- and cross-covariances between $1° \times 1°$ and $5° \times 5°$ anomaly blocks with distance $\psi$.

Before proceeding further with a description of each data set, it is necessary to define the area selected for the anomaly recovery. The basic criterion for the location of this area is the coverage of the altimetry data available at the time the computer programs were being developed and tested. This preprocessed data, free of systematic bias and orbit errors to within 78 cm, were made available to us by Professor Rapp[12] of The Ohio State University. The best coverage of these data was in a $5° \times 5°$ equal-area block whose latitude and longitude bounds are 40°-35° N and 291°-297° E, respectively. This block, which is approximately equivalent to a cap of radius $\psi = 2°.5$ (Figure 1), is within the calibration area.

For $\psi_{OM}$ in Figure 1, a value of 3° is chosen, which corresponds to a truncation error of about 1.5 mgals on the anomalies to be computed. This value is taken from the graph on page 23 of Reference (1) and corresponds to Standard Earth (SE)II[13] potential coefficients truncated at degree 16. Considering the improved Goddard Earth Model (GEM) 9[14] used in this study, this error of 1.5 mgals should be a very conservative estimate.

In the case of the truncation cap angle, $\psi_{OS}$, for the Stokes' formula, a value of 22 degrees which corresponds to a truncation error of just over 0.6 m is chosen.[1] Once again, this error corresponds to the SE II potential coefficients truncated at degree 16. Consequently, the outer circle (III) is of radius $27°.5$; the radius of the middle circle is $5°.5$ and that of the inner circle is $2°.5$. Assuming for practical purposes square areas instead of circular caps, terrestrial anomalies are required over a $55° \times 55°$ block and the altimetry data would be required over a $11° \times 11°$ block.

## 3.1 Altimetry Data

These data are taken from a set of sea surface topography heights and their standard errors in the GEOS-3 calibration area, supplied by Rapp[8]. The data are derived from the raw altimeter data corrected for tides and are free of bias and orbit errors to about 65 cm in the calibration area[8]. There are about 15,000 observations within the 11° x 11° area selected for this study. However, the maximum number of observations used in this study is 7475, taking every other observation. The geographical distribution of these data is as shown in Figure 2. This data set also had geoid undulations implied by the GEM-9 potential coefficients set truncated at degree 20.

## 3.2 Terrestrial Gravity Data

The anomaly data used in this study consist of two sets. The 5° x 5° equal-area anomalies and their standard errors were taken from Appendix A of Reference (7); the 1° x 1° (approximately) equal-area anomalies and their standard errors were supplied by Rapp from his tape called "August 1976 Tape"[7]. These anomalies are referred to the Geodetic Reference System 1967[15].

## 3.3 Spherical Harmonic Potential Coefficients

These data are a set of fully normalized potential coefficients complete to degree and order 20 from the GEM-9[14] and referred to the Geodetic Reference System 1967[15].

## 3.4 Numerical Autocovariance Model

The sizes of the blocks of anomalies involved in the recovery of 1° x 1° anomalies are 5 and 1 degrees. The autocovariance models for 1° x 1° anomalies and 5° x 5° anomalies and their cross-covariances are computed using the subroutine COVA[10], which uses the assumption that by varying

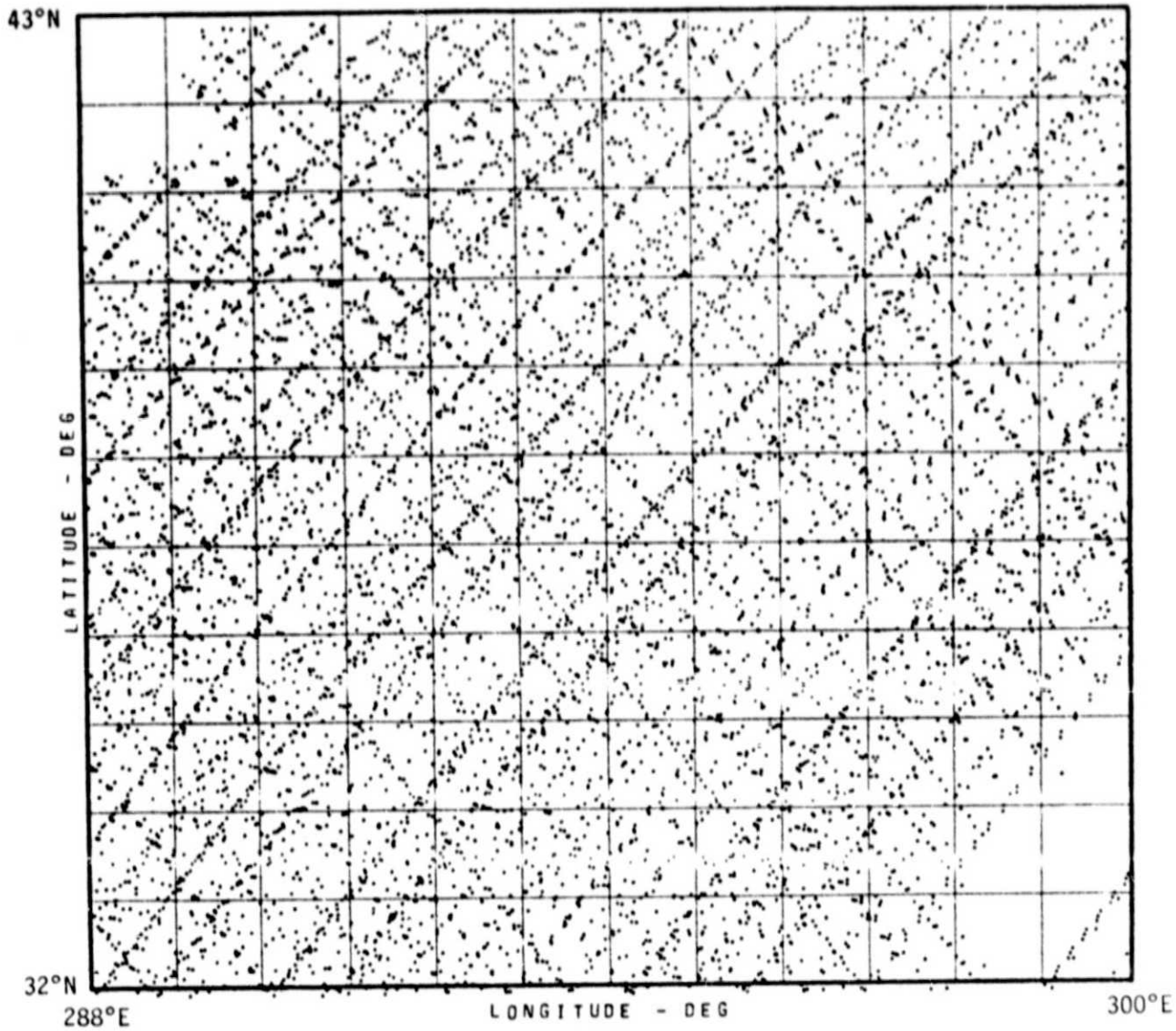


FIGURE 2. DISTRIBUTION OF ALTIMETER DATA

the heights of the points P and Q in the point anomaly autocovariance function C(P,Q) points $Q_1$ and $Q_2$ can be found, for which anomaly covariance $C(Q_1,Q_2)$ gives a good approximation to any (say 1° x 1°) mean anomaly covariance function. For example, $Q_1 = Q_2 = 10.4$ km will give covariances for 1° x 1° mean anomalies. Similarly, 5° x 5° mean anomaly covariances can be approximated by $C(Q_1, Q_1)$ for $Q_1 = 98.45$ km[16]. The cross-covariance between the 1° x 1° and the 5° x 5° mean anomalies are computed by setting $Q_1 = 10.4$ km and $Q_2 = 98.45$ km. A set of these covariances and cross-covariances computed by COVA for various angular distances, $\psi$, are given in Table 1 for Nmax = 20.

TABLE 1. MEAN ANOMALY COVARIANCES AND CROSS-COVARIANCES FOR 1-DEG AND 5-DEG BLOCKS

| $\psi$(deg) | 1x1 Deg (mgal$^2$) | 1x5 Deg (mgal$^2$) | 5x5 Deg (mgal$^2$) |
|---|---|---|---|
| 0.00 | 654.41 | 208.81 | 103.64 |
| .50 | 433.78 | 190.95 | 98.83 |
| 1.00 | 268.48 | 152.46 | 86.28 |
| 1.50 | 170.20 | 112.55 | 69.89 |
| 2.00 | 105.90 | 78.30 | 52.95 |
| 2.50 | 61.43 | 50.72 | 37.31 |
| 3.00 | 29.83 | 29.10 | 23.78 |
| 3.50 | 7.17 | 12.47 | 12.57 |
| 4.00 | -8.95 | -.06 | 3.59 |
| 6.00 | -33.78 | -22.18 | -14.31 |
| 8.00 | -26.93 | -19.60 | -14.08 |
| 10.00 | -10.69 | -8.55 | -6.70 |
| 12.00 | 3.54 | 1.90 | .90 |
| 14.00 | 10.72 | 7.52 | 5.24 |
| 16.00 | 10.48 | 7.68 | 5.61 |
| 18.00 | 5.41 | 4.15 | 3.17 |
| 20.00 | -.81 | -.38 | -.13 |
| 22.00 | -5.09 | -3.61 | -2.55 |
| 24.00 | -5.98 | -4.37 | -3.19 |
| 26.00 | -3.84 | -2.89 | -2.16 |
| 28.00 | -.29 | -.31 | -.29 |
| 30.00 | 2.74 | 1.94 | 1.38 |
| 35.00 | 2.02 | 1.53 | 1.15 |
| 40.00 | -2.76 | -2.01 | -1.46 |
| 45.00 | -.17 | -.16 | -.14 |
| 50.00 | 2.13 | 1.57 | 1.15 |

## 4. 1° x 1° MEAN GRAVITY ANOMALY RECOVERY

Since this study is a continuation of that reported in Reference (1), a brief summary of the previous results and conclusions may be helpful before presenting the results of the current study. The previous study was based purely on simulations where there were only one altimeter observation per block (1°x1°) over a 30° x 30° area. Mean anomalies over 1° x 1° blocks were recovered from these observations in a 10° x 10° area.

The highlights of the results were that:

(1) The recovery of 1° x 1° mean gravity anomalies was feasible with the procedure outlined earlier in this report

(2) A posteriori estimates for standard deviations obtained from the density of observations used (one per block) were about 19 mgal.

(3) Exclusion of the anomalies in the outer zone (Figure 1) as unknowns resulted in modeling errors (aliasing effect) being introduced in the anomalies being recovered; however, the aliasing effect on the a posteriori standard deviations was not very significant

(4) When these anomalies were included, the system of equations became unstable so that (a priori) wieghted constraints were necessary for any realistic results

(5) Minimum requirement for the density of observations was one per block.

These results form the basis for this study.

The major difference between the two studies is that the current study uses very dense real data while the previous study was based on simulation data which were very sparse. Consequently, the present study will attempt to examine several issues raised at the conclusion of the last study. The Principal issues include:

(1) The performance of the technique and procedure with real data

(2) The effect of the high density data on accuracy estimates of the anomalies recovered

(3) The use of mean anomalies of larger blocks in the outer and middle zones (Figure 1)

(4) The use of numerical auto- and cross-covariances for weighted constraints on the anomaly parameters.

It was hoped that answers to these issues would help in the formulation of an optimum procedure for improving our knowledge of the geopotential field using satellite altimeter data.

## 4.1 Mean Anomaly Parameter Systems

With the cap sizes chosen (in Section 3) for a non-global solution, the parameters will include all the equal-area mean anomalies within the area of a 55° x 55° equal-area block. This will result in 3025 1° x 1° equal-area mean anomalies, which is too large and expensive to handle for several tests to be performed in this study. Consequently, 5° x 5° equal-area mean anomalies are considered for the outermost 20° of the outer zone and 1° x 1° anomalies for the rest of the area, as shown in Figure 3, where the extent of the altimeter data is shown with the rectangle with broken lines. As a result, the total number of anomaly parameters would be 337 (112 - 5° and 225 - 1°). In the other tests, 5° anomalies are considered for both the middle and outer zones, in which case the number of anomaly parameters is 145 (120 - 5° and 25 - 1°). In the ensuing discussions, the system with 337 anomaly parameters will be referred to as System A, and System B would be that with 145 anomalies. It should be noted that there would be one error model parameter, $N_o$, to be determined in addition to the anomaly parameters.

## 4.2 A Priori Weights For The Parameters

The a priori weight matrix $P_x$ in Equation (12) can be considered to consist of two submatrices, given by:

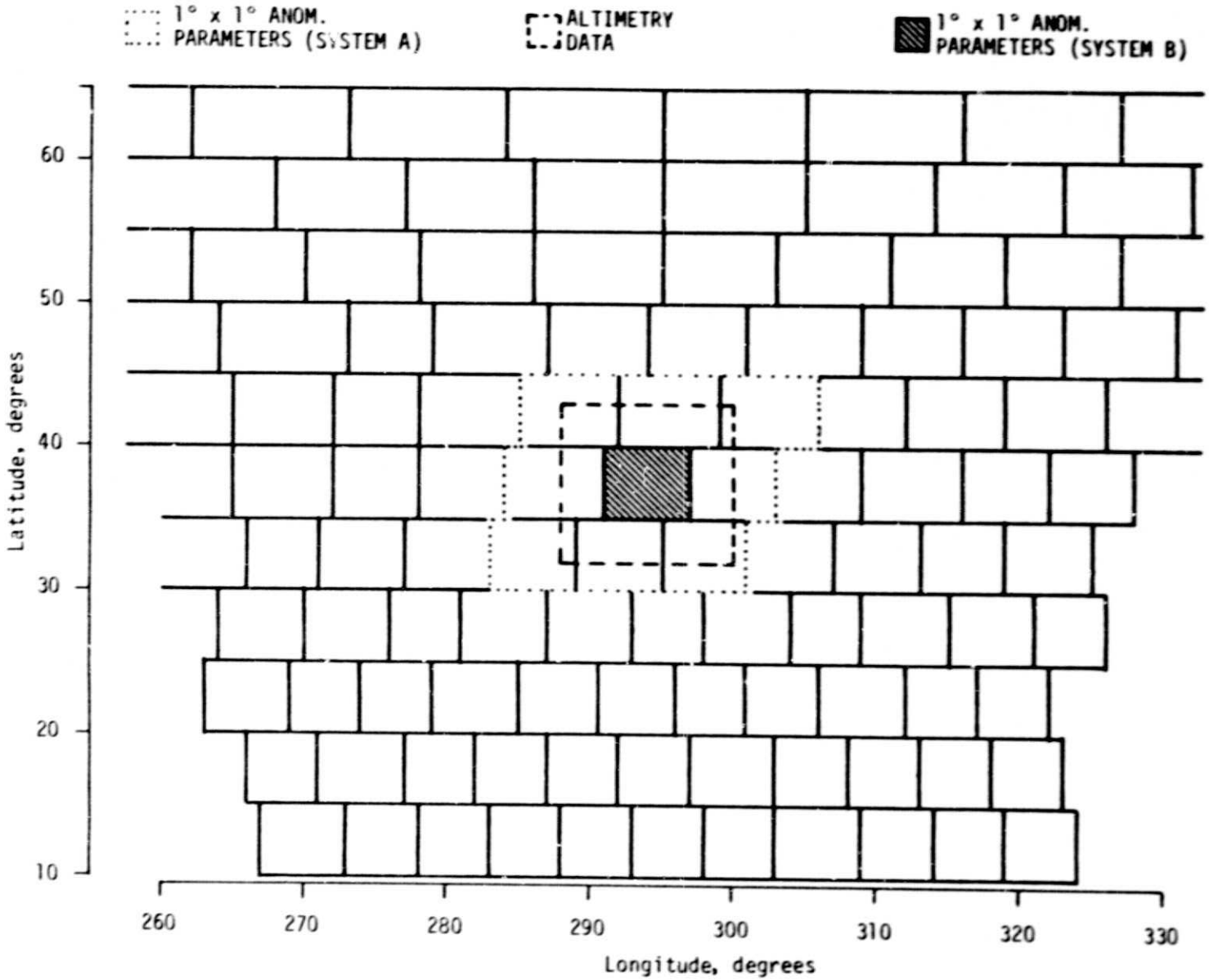


FIGURE 3. SYSTEM OF EQUAL AREA MEAN ANOMALY PARAMETERS

$$P_x = \begin{bmatrix} P_{\delta g} & 0 \\ 0 & P_{N_o} \end{bmatrix}, \tag{18}$$

implying that correlation between the residual anomalies $\delta g$ and $N_o$ are zero.

There are several ways the weight matrix $P_{\delta g}$ for the anomaly parameters can be defined, depending on the type of a priori information available on them. In the ensuing test for the mean anomaly computations, $P_{\delta g}$ is defined in four ways:

(1) It is set to zero ($P_{\delta g} = 0$), implying that we have no information on them.

(2) Using the estimates provided by Rapp[7] for the standard errors of the anomaly values determined from terrestrial measurements, $P_{\delta g}$ is defined as a diagonal matrix $D^{-1}$ where the elements of D are the square of the standard errors. That is:

$$P_{\delta g} = D^{-1} , \tag{19}$$

implying that the anomaly estimates are independent of each other.

(3) Assuming that the anomalies are stochastic quantities, their weight matrix is defined using the auto- and cross-covariances among them interpolated from the values presented in Table 1. If the auto- and cross-covariance matrix is C, then:

$$P_{\delta g} = C^{-1} . \tag{20}$$

(4) If the terrestrial estimates are assumed to consist of signals and noise[17], then:

$$P_{\delta g} = (C+D)^{-1} , \tag{21}$$

where C is the auto- and cross-covariance matrix and D is a error covariance matrix assumed diagonal as in Item (2) above.

For the purpose of determining the a priori weight for the constant, $N_o$, term, any error in $N_o$ is considered to come from two major sources:

(a) Uncertainty in the semimajor axis of the mean Earth ellipsoid

(b) Uncertainty in the equatorial gravity.

The accuracy estimate for the semimajor axis is given by Rapp[18] as 2.5 m. The error contribution from an uncertainty of 1 mgal in the equational gravity for a cap of 20° is about 2.6 m.[9] Therefore, the error due to both sources is 3.6 m, which, rounded to 4 m is used for the accuracy of $N_o$-term. Consequently,

$$P_{N_o} = 1/16 \text{ m}^{-2} . \tag{22}$$

For a priori values of anomalies, the terrestrial data described in Section 3.2 are used when $P_{\delta g}$ is defined according to Equations (19) and (21). Satellite anomalies as defined by Equation (6) are used when $P_{\delta g}$ is either 0 or $C^{-1}$. However, in all the ensuing computations, the a priori value for $N_o$ is assumed to be zero.

## 4.3 Tests With "Profile" Altimetry Data

At the time of the computer programs being modified/extended to accommodate the real data, it was decided to test them with the only pre-processed altimetry data available in the literature[12]. These data, which will be referred to as the profile data, were supplied to us on computer cards by Rapp. The distribution of these data (in the calibration area) is shown on Figure 4. It can be seen from this figure that only five passes are within the block where the gravity anomalies are sought.

The system of gravity anomalies assumed for these tests is System B, shown on Figure 3, where the total number of unknowns is 146. Four tests were carried out with the weight matrices $P_{\delta g}$ as described in the last section.

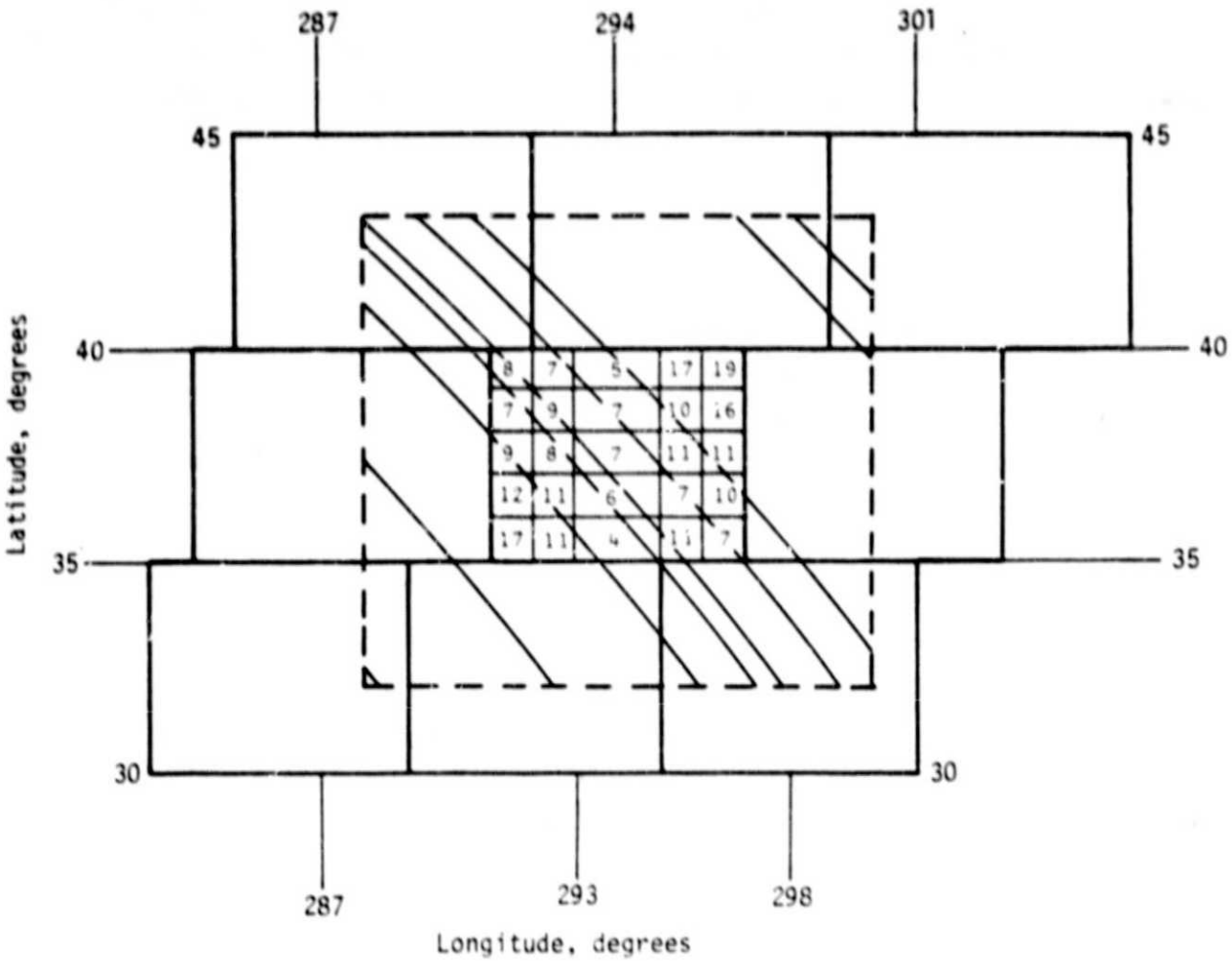


FIGURE 4. DISTRIBUTION OF THE TEST ("PROFILE") ALTIMETER DATA

In the first test where $P_{\delta g}$ was set to zero, the system of normal equations was unstable. The results of the other three tests are summarized in Table 2, where the blocks in which there are no altimeter data available are excluded. In this table, the average a priori standard deviation and the average a posteriori standard deviation are self-explanatory. The Root Mean Square (RMS) anomaly difference refers to the difference between the terrestrial anomaly estimates and those computed in these tests. The results of Table 2 show that there is very little difference between the three weighting procedures. However, comparing the recovered anomalies in each of these tests, we find that while the RMS difference between the tests where $P_{\delta g} = (C+D)^{-1}$ and $P_{\delta g} = C^{-1}$ is only about 3 mgal, it is about 12 mgal for the test where $P_{\delta g} = D^{-1}$ and each of the other two. This indicates the strong possibility that the a priori relative weights for the anomalies which are computed from terrestrial estimates are incorrect.

How much of an improvement these anomalies obtain in their estimates from the altimeter data is demonstrated in Figure 4, where the a posteriori standard deviations[16] corresponding to the case of $P_{\delta g} = C^{-1}$ are given. These numbers show that the anomalies of blocks where there are no altimeter data are very poorly determined. Their determination is best when the altimeter pass goes through the center of the block or when the data are dense and uniformly distributed within the block.

TABLE 2. RESULTS OF ANOMALY RECOVERY WITH "PROFILE" DATA

| Statistical Parameter | $P_{\delta g} = (C+D)^{-1}$ | $P_{\delta g} = C^{-1}$ | $P_{\delta g} = D^{-1}$ |
|---|---|---|---|
| Average standard deviation (1σ), mgal | | | |
| A priori | 28.1 | 26.3 | 10.0 |
| A posteriori | 9.1 | 8.4 | 7.2 |
| RMS difference with terrestrial anomaly, mgal | 16.3 | 16.8 | 16.4 |
| Variance of unit weight ($\hat{\sigma}_o$) | 0.86 | 0.85 | 1.08 |
| Constant $N_o$, m | -7.0 ± 1.4 | -5.1 ± 1.2 | -2.1 ± 0.7 |

## 4.4 Tests With Low Density Altimeter Data

The term low density refers to the set of 1496 data points which is one of every five data points shown on Figure 2. The difference between this and the profile data as discussed in the last section is that the low-density data are more evenly distributed in the area than the profile set. In order to study the effects of these low-density data on this anomaly recovery, three more sets of computations were made with the same System (E) of anomaly unknowns. Since the difference between using $P_{\delta g} = C^{-1}$ and $P_{\delta g} = (C+D)^{-1}$ is small, as seen from the previous tests, it was decided that the three new determinations would use:

(a) $P_{\delta g} = 0$

(b) $P_{\delta g} = (C+D)^{-1}$

(c) $P_{\delta g} = D^{-1}$ .

The results of these determinations are summarized in Table 3.

TABLE 3. RESULTS OF ANOMALY RECOVERY WITH LOW DENSITY DATA

| Statistical Parameter | $P_{\delta g} = 0$ | $P_{\delta g} = (C+D)^{-1}$ | $P_{\delta g} = D^{-1}$ |
|---|---|---|---|
| Average standard deviation (1σ), mgal | | | |
| A priori | ∞ | 28.1 | 10.0 |
| A posteriori | 5.7 | 6.0 | 6.1 |
| RMS difference with terrestrial anomaly, mgal | 14.8 | 13.2 | 13.0 |
| Variance of unit weight ($\hat{\sigma}_o$) | 1.06 | 1.24 | 1.62 |
| Constant $N_o$, m | 0.7 ± 4.1 | -3.6 ± 2.3 | 0.5 ± 1.0 |

Once again, on the average, there is very little difference between results of the various weighting procedures. Results in Table 3 indicate that the a posteriori standard deviation estimates as well as the RMS difference between the computed and terrestrial anomalies have improved somewhat over

those with the profile data. Also, the RMS differences between the anomalies determined with $P_{\delta g} = (C+D)^{-1}$ and $P_{\delta g} = D^{-1}$ have dropped to 7.5 mgal compared to 12 mgal with the profile data. In fact, the difference is less than 5 mgal for 19 of the 25 anomalies computed. However, the reasons for the differences of greater than 10 mgal in the other six anomalies are not clear at this time. It should also be noted that the system of normal equations appears to be stable for $P_{\delta g} = 0$ for the anomaly and altimetry data systems under consideration.

## 4.5 Tests With High Density Data

In these tests, the altimeter data used are as shown on Figure 2, (7475 data points) which is five times denser than the low-density data discussed in the last subsection. These tests are aimed at examining the effect of high-density data on the accuracy estimates of the anomalies being determined. Here again we use the same weighting functions and the anomaly parameter System B that were used with the low-density data. The results corresponding to these tests are given in Table 4.

TABLE 4. RESULTS OF ANOMALY RECOVERY WITH HIGH DENSITY DATA

| Statistical Parameter | $P_{\delta g} = 0$ | $P_{\delta g} = (C+D)^{-1}$ | $P_{\delta g} = D^{-1}$ |
|---|---|---|---|
| Average standard deviation (1σ), mgal | | | |
| A priori | ∞ | 28.1 | 10.0 |
| A posteriori | 2.6 | 2.5 | 2.7 |
| RMS difference with terrestrial anomaly, mgal | 14.8 | 14.3 | 14.1 |
| Variance of unit weight ($\hat{\sigma}_o$) | 1.06 | 1.13 | 1.34 |
| Constant $N_o$, m | 2.4 ± 3.5 | 4.8 ± 1.9 | 0.37 ± 0.8 |

This is again another example of the consistent agreement among the various weighting algorithms. The dominance of the altimeter data can be seen from agreement between the computed anomalies under the various weighting procedures. The RMS difference for the cases $P_{\delta g} = 0$ and $P_{\delta g} = (C+D)^{-1}$ is 8.6 mgal. For the cases $P_{\delta g} = (C+D)^{-1}$ and $P_{\delta g} = D^{-1}$, this difference is only 4 mgal. Comparing the results of the high-density data with those of the low-density data, the estimated standard deviation averaged for the 25 blocks is just under half fo. fi:e times increase in the density of altimeter data. The RMS difference in the computed anomalies is only 4.6 mgal.

## 4.6 Tests With 1° x 1° Anomalies of System A

The anomaly System A (Figure 3) consists of 1° x 1° anomalies extending 2 degrees beyond the middle zone (Figure 1). The total number of anomaly parameters in this system is 337, of which 225 are 1° x 1° anomalies. The number of observations corresponding to the high-density data is 7475. Computer timewise, it would be very expensive to use the high-density data with the system of 338 unknowns including th. $N_o$-term. Consequently, we decided to examine the effect of extending the 1° x 1° anomalies beyond the middle zone with the low-density data which has 1496 data points. The weighting functions remained the same. The results are summarized in Table 5.

TABLE 5. RESULTS OF ANOMALY RECOVERY FOR ANOMALY SYSTEM A

| Statistical Parameter | $P_{\delta g} = 0$ | $P_{\delta g} = (C+D)^{-1}$ | $P_{\delta g} = D^{-1}$ |
|---|---|---|---|
| Average standard deviation (1σ), mgal | | | |
| A priori | ∞ | 28.1 | 10.0 |
| A posteriori | 23.4 | 4.4 | 3.9 |
| RMS difference with terrestrial anomaly, mgal | 19.0 | 11.7 | 10.5 |
| Variance of unit weight ($\hat{\sigma}_o$) | 0.72 | 0.82 | 0.93 |
| Constant $N_o$, m | 0.1 ± 2.9 | -4.8 ± 1.6 | -7.8 ± 0.6 |

Unlike with the anomaly System B, the system of normal equations is unstable for zero a priori weights on the anomalies. The RMS difference between the computed and the terrestrial anomalies is the lowest (about 11 mgal) among all the different sets of computations we have done in this study.

The effect of extending the smaller anomaly blocks (1° x 1°) beyond the middle zone can be best seen in a comparison in Table 6 between the results obtained with Systems A and B. The weighting function used in this comparison is $(C+D)^{-1}$.

TABLE 6. COMPARISON OF RESULTS WITH SYSTEMS A AND B

| Statistical Parameter | System A | System B |
|---|---|---|
| Average a posteriori standard deviation (1σ), mgal | 4.4 | 6.0 |
| RMS difference with terrestrial anomaly, mgal | 11.7 | 13.2 |
| RMS difference with $P_{\delta g} = D^{-1}$, mgal | 5.8 | 7.5 |
| Variance of unit weight ($\hat{\sigma}_o$) | 0.82 | 1.24 |
| Constant $N_o$, m | -4.8 ± 1.6 | -3.6 ± 2.3 |
| RMS difference (A-B) | 9.8 mgal | |

The results in this table demonstrate the overall improvement in performance with System A when compared with System B. Yet, the differences are not dramatic. However, the anomalies recovered in both the systems are significantly different (RMS difference = 9.8 mgal) but still consistent with the accuracy estimates associated with the anomalies. Most of this difference could be attributed to the aliasing effect resulting from approximating the detailed anomalous gravity structure in the middle zone with larger block anomalies.

The accuracy estimates (4.4 mgal) obtained with low-density data are excellent considering the accuracy of the terrestrial data available

today. This estimate can be further improved to about 2-2.5 mgal with the high-density data, as we have seen with the results with the anomaly System B (Table 4).

## 4.7 Comparison With Rapp's Anomalies

In order to determine how good these computed anomalies are, we provide the following comparison in Figure 5. Four candidate sets of anomalies are selected for this comparison:

(1) Set 1 - This set corresponds to System A, as discussed in the last subsection, with a priori weights $P_{\delta g} = (C+D)^{-1}$. In this system, 1° x 1° anomaly unknowns extended 2° bevond the middle zone.

(2) Set 2 - This corresponds to System B with 5° x 5° anomalies used for the middle and outer zones, and high density altimetry data. Again, the weighting function is $(C+D)^{-1}$.

(3) Rapp's anomalies - computed using Least-Squares collocation techniques[2,19]. These anomalies correspond to 1° x 1° equiangular blocks. The difference between the equiangular and equal-area blocks in the area under consideration is that two equiangular blocks form an equal-area block within a 2° longitudinal band in the middle of the 5° x 5° equal-area block, as shown in Figure 5. In such cases, equal-area anomalies are derived from averaging the equiangular anomalies and accuracy estimates.

(4) Terrestrial anomalies - as described in Subsection 3.2.

Quantitative differences among the various anomaly sets compared are computed in the form of RMS differences and shown in Table 7. The larger differences occur with Set 2 and the smallest one is between Rapp's and ter estrial anomalies followed closely by Set 1/Rapp differences. In a further look at the differences between Set 1 and Rapp's anomalies, it was found that significantly large differences occur in the blocks where the

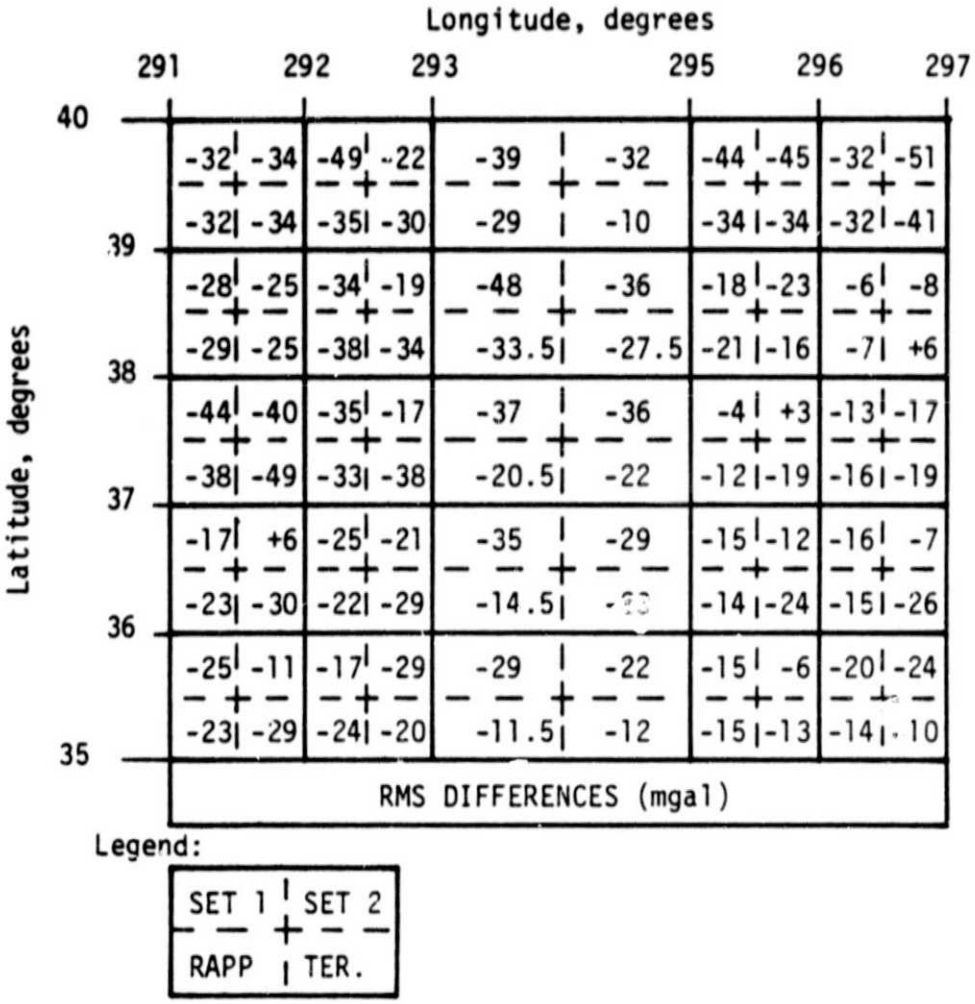


FIGURE 5. COMPARISON OF COMPUTED ANOMALIES

equiangular anomalies had to be averaged to get equal-area anomalies. Consequently, we compared the two sets again excluding these five blocks, and the agreement is significantly improved (5.4 mgal). Similar comparison between Set 1 and terrestrial anomalies shows the same improvement (8.7 mgal). The larger differences in these five blocks may perhaps be due to the fact that the equal-area blocks are not equal area at all and the equiangular blocks are, in fact, equal area in a non-global solution. Consequently, the 1° x 1° covariance function is improperly used for 1° x 2° blocks. However, this effect is considerably reduced by the dominance of the high-density altimeter data as we have seen with System B.

An accuracy estimate of 2.5 mgal was obtained for 1° x 1° equal-area anomalies with the high-density altimetry data. The corresponding estimates for terrestrial data is 10 mgal and 7.3 mgal for Rapp's[19].

TABLE 7. RMS DIFFERENCES BETWEEN THE ANOMALY SETS

| Anomaly Set | RMS Differences (mgal) |
|---|---|
| Set 1 - Set 2 | 9.8 |
| Set 1 - Rapp | 8.7 |
| Set 1 - terrestrial | 11.7 |
| Set 2 - Rapp | 11.4 |
| Set 2 - terrestrial | 13.2 |
| Rapp - terrestrial | 7.5 |
| Rapp - Set 1 (20 equiangular blocks only) | 5.4 |
| Set 1 - terrestrial (20 equiangular blocks only) | 8.7 |

## 4.8 Summary of 1° x 1° Anomaly Recovery

As outlined at the outset of this chapter, we examined three aspects of the determination of gravity anomalies from real altimetry data:

(1) The effect of data distribution on the accuracy of the anomalies determined

(2) The effect of substituting smaller blocks for the larger blocks within the middle and outer zones

(3) Use of auto- and cross-covariances for gravity anomalies as a priori weighting functions.

The results can be summarized as follows:

(1) It has been demonstrated that the technique and procedures used here can be used effectively with real altimetry data in the recovery of 1° x 1° mean gravity anomalies.

(2) Realistic estimates for these anomalies can be determined with varying degrees of accuracy depending on the density and distribution of the altimetry data

(3) When the density of observation is low or if only a few profiles of altimeter data are available, the use of auto- and cross-covariance functions as a priori weights can result in improved anomaly estimates. However, the anomaly blocks should have at least one profile passing through for any significant improvement in the anomaly estimates from altimetry data.

(4) The use of larger anomaly blocks in the middle and outer zones to reduce the number of parameters results in significantly large aliasing effect/model errors introduced in the anomalies being sought within the inner zone. However, the use of 1° x 1° blocks to at least 2 to 3 degrees beyond the middle zone and 5° x 5° blocks in the rest of the outer zone may be optimum in the sense that the number of parameters would

be small enough for practical purposes and at the same time the resulting aliasing effect would be small enough to be neglected.

(5) 1° x 1° mean anomalies can be recovered to about 4.4 mgal accuracy with low-density data (one of every five observations shown in Figure 2). This accuracy can be increased to 2-2.5 mgal with high-density data (all data points shown on Figure 2).

(6) The anomaly set considered to be the most realistic of those computed in this study compares very well with Rapp's estimates and with the terrestrial estimates. The accuracy estimates obtained both with low- and high-density data show considerable improvement over Rapp's as well as those of the terrestrial estimates.

These comparisons, however, are meaningless unless we have ground truth data with an accuracy better than the 2-2.5 mgal accuracy claimed in this study to verify the validity of these claims. Until then, we can only say that the results obtained in this study are comparable with, if not superior to, the best estimates available today.

## 5. 30' x 30' MEAN ANOMALY RECOVERY

It may be recalled that the objective of this study is to develop practical applications for the high resolution altimeter capability of GEOS-3 and future SEASAT satellite missions, with the primary effort being the development and test of suitable techniques for gravity anomaly determination in the marine area which is one of such applications. We have effectively demonstrated the Least-Squares technique in recovering 1° x 1° equal-area mean anomalies from both the low and high density altimetry data. Now, it remains to be seen whether this technique can be used to resolve finer structures of the gravity field from the high density altimeter data. In the ensuing discussions, we will present some preliminary results of a 30' x 30' mean anomaly determination.

### 5.1 Parameter System For The 30' x 30' Anomaly Recovery

The high density data were used in determining the 30' x 30' mean anomalies. In order to keep the number of data points and the number of parameters in the system low for economical reasons, we decided to recover 36 30' x 30' approximately equal-area mean anomalies in a 3° x 4° block bounded by latitudes 36°-39° north and longitudes 292°-296° east (Figure 6). These blocks were subdivided from nine 1° x 1° equal-area (approximate) blocks which were used in the 1° x 1° anomaly recovery. High density altimeter data from a 5° x 5° equal-area block (1858 data points) are used for this computation. As can be seen from Figure 6, these data extend 1 degree beyond the inner zone in which the anomalies are sought.

In the middle zone, which is a band of 1 degree around the inner zone, 1° x 1° anomalies are used with another 20-degree band of 5° x 5° anomalies in the outer zone. This system results in 132 anomaly parameters and one error model parameter $N_o$.

### 5.2 A Priori Information On The Anomalies

Since terrestrial estimates for the 30' x 30' blocks were not readily available, the terrestrial value of the 1° x 1° block of which the

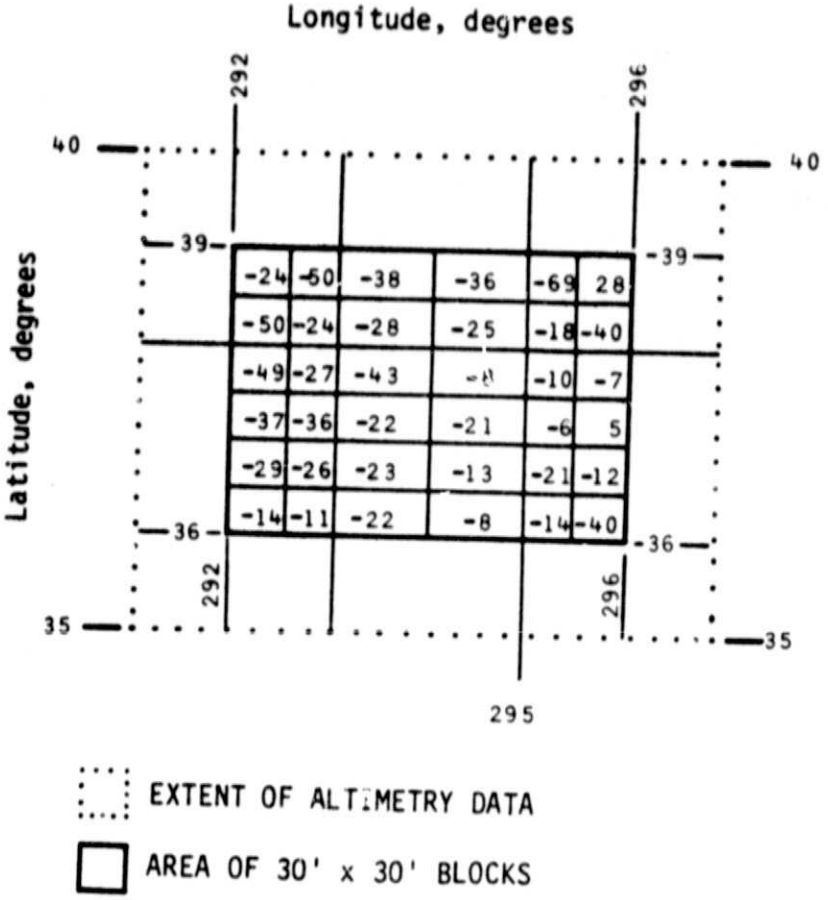


FIGURE 6. EQUAL AREA (APPROXIMATE) BLOCK SUBDIVISION FOR 30' x 30' MEAN ANOMALY RECOVERY

30' x 30' blocks were subdivisions were used for all the four subdivisions. Terrestrial estimates were used for the 1° x 1° and 5° x 5° blocks.

Equation (19), $P_{\delta g} = D^{-1}$ model, was used for weighting the anomalies where the elements corresponding to the 30' x 30' blocks were set to zero. Auto- and cross-covariance models were not used since they were not readily available. However, an approximate model could be computed with the subroutine COVA[16] employing the approach used by Tscherning and Rapp[16]. This approach uses the similarities between the smoothing operator $\beta_\ell$ and $\left(\frac{R_e}{R_e+h_Q}\right)^{\ell+2}$, where $R_e$ is the average Earth radius and $h_Q$, the height of a point above the Earth such that a point covariance function C(Q,Q) will adequately approximate the covariance function of $\theta° \times \theta°$ block anomalies.

$\beta_\ell$ can be expressed in terms of the radius $\psi_o$ of a circular cap as:

$$\beta_\ell = \frac{1}{1-\cos\psi_o}\ \frac{1}{2\ell+1}\left[P_{\ell-1}(\cos\psi_o) - P_{\ell+1}(\cos\psi_o)\right], \qquad (23)$$

where $P_\ell$ is the Legendre Polynomial of degree $\ell$. Now, $\psi_o$ can be approximated equating the area of circular and square caps; that is, $\psi_o = \frac{\theta^o}{\sqrt{\pi}}$. For 30' x 30' blocks, $\theta = 0.5$. Thus, knowing the values of $\beta_\ell$, a value of $h_Q$ could be found such that:

$$\beta_\ell = \left(\frac{R_e}{R_e+h_Q}\right)^{\ell+2} \qquad (24)$$

for all $\ell$. Then $h_Q$ can be used as an input for the subroutine COVA to compute the numerical auto- and cross-covariance model. Because of limitations of time and resources in this project, however, computations of these covariances could not be accomplished.

## 5.3 Results and Discussion

The 30' x 30' mean anomalies as computed with high density altimeter data are presented in Figure 6. Their average standard deviation ($1\sigma$) was 5 mgal with the estimate of the variance of unit weight being 0.6. The error model parameter $N_o$ was estimated to be - 1.76 ± 0.5 meters.

These numbers look very realistic except in the upper right corner of Figure 6, where unusually high and low(-69 and 28) values are noted in the adjoining blocks. A closer look at Figure 2 indicates that this block has poor "across the track" data coverage. These values may be due to that; on the other hand, they may be reasonable. Only good ground truth data can resolve such questions.

As we mentioned earlier, the terrestrial estimates for these anomalies were not readily available for comparison at the time this report was written. However, 1° x 1° mean anomalies are averaged from these 30' x 30' anomalies and compared with those from Figure 5 corresponding to Set 1, Rapp's, and the terrestrial sets. The results of this comparison is provided in Table 8 in the form of RMS differences. In the comparison with Set 1, the larger blocks, where unusually larger differences due to improper covariance function were noted, were excluded.

TABLE 8. COMPARISON WITH OTHER ANOMALY SETS

| Averaged 1° x 1° Anomaly Minus | RMS Differences (mgal) |
|---|---|
| Terrestrial | 6.7 |
| Rapp | 4.4 |
| Set 1 (Figure 5) | 4.8 |

These comparisons are very good considering the standard deviations associated with them. However, this agreement is not an indication

that the individual 30' x 30' mean anomalies obtained in these computations are resolved with good accuracy, but it certainly indicates that the estimates are very realistic. Accurate ground truth data are required to verify these estimates.

The accuracy of 5 mgal for the 30' x 30' anomalies is excellent considering the data distribution, which is poor in the direction across the track (satellite pass). It would be informative to see how the more uniformly distributed data expected from the SEASAT missions will affect these accuracy estimates.

## 6. CONCLUSIONS AND RECOMMENDATIONS

The results of the study presented in Sections 5 and 6 of this report led to the following conclusions:

(1) The technique and procedures developed and used in this study are very effective in the determination of detailed mean gravity anomalies to the extent of 1° x 1° and 30' x 30' blocks.

(2) The accuracy estimates for the computed anomalies are highly dependent on the density and distribution of data points.

(3) The anomalies computed are sensitive to a priori relative weights used as constraints. This sensitivity reduces with increased density and uniform distribution of the data points.

(4) The use of the accuracy estimates given for the terrestrial anomalies for a priori weight constraints results in poor relative weights among the anomalies.

(5) The use of auto- and cross-covariance models for anomalies as a priori weight constraints is very effective in determining realistic anomaly estimates when the density of data points is low or if only a few profiles of altimetry data are available in the area.

(6) A block should have at least one profile passing through it for any significant improvement in the estimate of its value.

(7) Approximation of small blocks by larger blocks in the middle and outer zones reduces the unknowns and increases the stability of the normal equation system. However, this introduces significant model errors/"aliasing" effect on the anomalies to be determined. As a compromise, the use of the small blocks in at least the middle zone results in a reasonable size of the parameter system and small modeling errors. In fact,

the small blocks were extended 2 degrees beyond the middle and into the outer zone in this study.

(8) When the auto- and cross-covariances are used for a priori weighted constraints, ideally the blocks where the anomalies are determined have to be truly equal in area. In a non-global solution, equiangular blocks would be approximately equal area. The equal-area subdivision, as used in this study, where some blocks are double the area of the others, results in improper relative weights. However, this needs to be examined further.

(9) With the low density data (1496 data points over a 11° x 12° block), 1° x 1° mean anomalies can be determined with an accuracy of about 4 mgal. Indications are that this figure can be improved to about 2 mgal with high density data (7475 data points). A preliminary determination showed that 30' x 30' mean anomalies can be estimated with an accuracy of about 5 mgal with the high density data.

(10) Computed anomalies compared well with those computed by Rapp using Least-Squares Collocation techniques and with terrestrial estimates; the accuracy estimates obtained in this study are significantly better. However, due to the lack of accurate ground truth data, we cannot verify how good each of these determinations is.

Even though significant results have been obtained considering the available time and resources in this study, there are several areas that need further examination. Some of these are listed below:

(1) Some of the equal-area blocks used here are larger than the other blocks due to the subdivision scheme used. The 1° x 1° autocovariances used for a priori weight constraints appear to have unfavorable effects on the anomaly estimates. These effects need to be examined by using either truly equal-area blocks or equiangular blocks.

(2) The 1° x 1° anomalies must be recomputed using high density data with Parameter System A, where the 1° x 1° anomaly parameters are extended 2° beyond the middle zone. This computation was not done in this study due to the limitations of time and resources.

(3) The data distribution in Figure 2 shows poor cross-track coverage. It would be instructive to see the effect of more uniform data coverage on the computed anomalies and their accuracy estimates.

(4) The anomaly parameter system used for the 30' x 30' anomaly determinations must be reexamined to see whether any improvement to the anomaly and their accuracy estimates could be made.

(5) The possibility of resolving mean anomalies over still smaller blocks (e.g., 15' x 15') must be examined.

(6) However improved the anomaly and the accuracy estimates may be, they are meaningless unless we can verify them with proper ground truth data. The ground truth data presently available are totally inadequate with respect to coverage and accuracy. There should be a concerted effort on the part of the agencies responsible for geodesy to establish a marine calibration range where proper ground truth data could be established for verifying the high resolution altimeter data and their derivatives.

## 7. REFERENCES


(1) Gopalapillai, S., "Non-Global Recovery of Gravity Anomalies From a Combination of Terrestrial And Satellite Altimetry Data", Reports of the Department of Geodetic Science, No. 210, The Ohio State University, Columbus, Ohio, July 1974.

(2) Rapp, R. H., "Gravity Anomaly Recovery From Satellite Altimetry Data Using Least Squares Collocation Techniques", Reports of the Department of Geodetic Science, No. 220, The Ohio State University, Columbus, Ohio, December 1974.

(3) Sjoberg, L., "Mean Gravity Anomaly Recovery From Altimeter Data Using Fourier Transforms", Reports of the Department of Geodetic Science (in press), The Ohio State University, Columbus, Ohio, 1977.

(4) Molodenskii, M. S., Eremeev, V. F., and Yurkina, M. I., Methods For Study of the External Gravitational Field And Figure of the Earth, Translated from Russian (1960), Israel Program of Scientific Translations, Jerusalem, 1962.

(5) Rummel, R, "The Determination of Gravity Anomalies From Geoid Heights Using the Inverse Stokes' Formula", Reports of the Department of Geodetic Science (in press), The Ohio State University, Columbus, Ohio, 1977.

(6) Heiskanen, W., and Moritz, H., Physical Geodesy, S. Freeman and Co., San Francisco, 1967.

(7) Rapp, R. H., "Potential Coefficient Determinations From 5° Terrestrial Gravity Data", Reports of the Department of Geodetic Science, No. 251, The Ohio State University, Columbus, Ohio, January 1977.

(8) Rapp, R. H., "Incomplete Final Results For Sea Surface Topography And Gravity Anomalies From GEOS-3 Altimeter Data", Proceedings of the GEOS-3 Conference, New Orleans, Louisiana, November 18-19, 1977.

(9) Rapp, R. H., and Rummel, R., "Methods For The Computation of Detailed Geoids And Their Accuracy", Reports of the Department of Geodetic Science, No. 233, The Ohio State University, Columbus, Ohio, November 1975.

(10) Levallois, J. J., "Calcul du Geoide Gravimetrique sur le Territore de la France", Communication presented to the XV General Assembly, International Union of Geodesy and Geophysics and International Association of Geodesy, Moscow, U.S.S.R., 1971.

(11) Talwani, M., Roppe, P. D., and Rokinowitz, P. D., "Gravimetrically Determined Geoid in the Western North Atlantic", Sea Surface Topography From Space, Technical Report ERL 228-ADML 7-2, Volume 2, National Oceanic And Atmospheric Administration, Washington, D.C., 1972.

(12) Rummel, R., and Rapp, R. H., "Undulation And Anomaly Estimation Using GEOS-3 Altimeter Data Without Precise Satellite Orbits", Bulletin Geodesique, 51 (1), 73-88 (1977).

(13) Gaposchkin, E. M., and Lambeck, K., "Earth's Gravity Field to the Sixteenth Degree And Station Coordinates From Satellite And Terrestrial Data", J. Geophys. Res., 76 (1971)

(14) Lerch, F. J., Klosko, S. M., Laubscher, R. E., and Wagner, C. A., "Gravity Model Improvement Using GEOS-3 (GEM-9 & 10)", Report No. X-921-77-246, Goddard Space Flight Center, Greenbelt, Maryland, September 1977.

(15) International Association of Geodesy (IAG), "Geodetic Reference System 1967", Special Publication of Bulletin Geodesique.

(16) Tscherning, C. C., and Rapp, R. H., "Closed Covariance Expressions For Gravity Anomalies, Geoid Undulations, and Deflections of the Vertical Implied by Anomaly Degree Variance Models", Reports of the Department of Geodetic Science, No. 208, The Ohio State University, Columbus, Ohio, May 1974.

(17) Moritz,H., "Advanced Least Squares Methods", Reports of the Department of Geodetic Science, No. 175, The Ohio State University, Columbus, Ohio, June 1972.

(18) Rapp, R. H., "Adjusted Parameters of the Mean Earth Ellepsoid", Proceedings of the International Symposium on Earth's Gravitational Field and Secular Variations in Position, Sydney, Australia, November 1973.

(19) Rapp, R. H., "Mean Gravity Anomalies And Sea Surface Heights Derived From GEOS-3 Altimeter Data", Reports of the Department of Geodetic Science, No. 268, The Ohio State University, Columbus, Ohio, December 1977.